eXPRESS Polymer Letters Vol.7, No.1 (2013) 95–105
Available online at www.expresspolymlett.com
DOI: 10.3144/expresspolymlett.2013.9

A versatile characterization of poly(*N*-isopropylacrylamide-co-*N*,*N*′-methylene-bis-acrylamide) hydrogels for composition, mechanical strength, and rheology

A. Chetty[1], *J. Kovács*[2], *Zs. Sulyok*[2], *Á. Mészáros*[3], *J. Fekete*[3], *A. Domján*[4], *A. Szilágyi*[2], *V. Vargha*[2*]

[1]CSIR Materials Science and Manufacturing, Polymers and Composites, PO Box 395, 0001 Pretoria, South Africa
[2]Budapest University of Technology and Economics, Department of Physical Chemistry and Materials Science, Műegyetem rkp. 3. H/1, H-1111 Budapest, Hungary
[3]Budapest University of Technology and Economics, Department of Inorganic and Analytical Chemistry, Műegyetem rkp. 3. Ch/A, H-1111 Budapest, Hungary
[4]NMR Spectroscopy Laboratory, Institute of Organic Chemistry, Research Centre for Natural Sciences ,Hungarian Academy of Sciences, Pusztaszeri út 59–67, H-1025 Budapest, Hungary

Received 26 June 2012; accepted in revised form 6 September 2012

Abstract. Poly(*N*-isopropylacrylamide-co-*N*,*N*′-methylene-bisacrylamide) (P(NIPAAm-co-MBA)) hydrogels were prepared in water using redox initiator. The copolymer composition at high conversion (>95%) was determined indirectly by HPLC (high performance liquid chromatography) analysis of the leaching water and directly by solid state ^{13}C CP MAS NMR (cross polarization magic angle spinning nuclear magnetic resonance) spectroscopy of the dried gels, and was found to be close to that of the feed. The effect of cross-linker (MBA) content in the copolymer was investigated in the concentration range of 1.1–9.1 mol% (R:90–10; R = mol NIPAAm/mol MBA) on the rheological behaviour and mechanical strength of the hydrogels. Both storage and loss modulus decreased with decreasing cross-linker content as revealed by dynamic rheometry. Gels R70 and R90 with very low cross-linker content (1.2–1.5 mol% MBA) have a very loose network structure, which is significantly different from those with higher cross-linker content manifesting in higher difference in storage modulus. The temperature dependence of the damping factor served the most accurate determination of the volume phase transition temperature, which was not affected by the cross-link density in the investigated range of MBA concentration. Gel R10 with highest cross-linker content (9.1 mol% MBA) behaves anomalously due to heterogeneity and the hindered conformation of the side chains of PNIPAAm.

Keywords: *polymer gels, PNIPAAm, rheology, mechanical properties, copolymer composition*

1. Introduction

Poly(*N*-isopropylacrylamide) (PNIPAAm) based hydrogels belong to the family of 'intelligent' materials, since they are able to undergo a volume phase transition at 32–34°C on the application of an external stimulus, namely change in temperature. By increasing the temperature the molecules of the polymer gel change their conformation from coil to globule resulting in a change in their hydrophilic-hydrophobic character. Many applications of these smart hydrogels are being investigated such as thermo-responsive membranes [1], efficient and reversible immobilization of biomacromolecules [2–5], *in vitro* cell cultivation [6], separation of lignin [7] or phenols from aqueous mixtures [8–10] and drug and gene delivery [11]. Some special uses such

*Corresponding author, e-mail: vvargha@mail.bme.hu

as biosensors [12], molecular imprinting [13], fluid microchips [14], as well as numerous biomedical applications are also being studied [3–5].

Since PNIPAAm homopolymer is water-soluble, for making hydrogels it must be cross-linked and for this purpose *N*,*N*′-methylene-bisacrylamide (MBA) is mostly used. The molar ratio of PNIPAAm and the cross-linker MBA in the feed composition is often expressed as R. The real ratio of the cross-linker in the copolymer however is hardly referred to in the literature. Further on cross-linking is purposed to improve the mechanical and elastic properties of the hydrogel. Dynamic rheometry provides important characterization with respect to linear viscoelasticity, strength, relaxational and phase transition of the material. In addition to the conventional methods, such as measuring the swelling ratio, turbidity measurements, calorimetry etc., dynamic rheometry also offers an alternative technique to accurately determine the volume phase transition of the gels. Petit and co-workers grafted PNIPAAm onto polyacrylamide backbone and investigated the thermoassociating properties of the graft copolymer by dynamic rheometry. Upon heating, PNIPAAm grafts dehydrate and self-aggregate into hydrophobic microdomains which promote the formation of a physical network above 36°C [15]. Senff and Richtering [16] investigated the effect of MBA cross-linker content on the rheological properties of PNIPAAm microgels. Zeng *et al*. [17] investigated the rheological behaviour of PNIPAAm homopolymer solutions in water during phase separation and proved the formation of physical network.

In this study P(NIPAAm) was cross-linked with MBA in the range of 1.10–9.10 mol% (R90–10). The copolymer composition at high conversion was determined directly by analyzing the resulted dry gels with solid state magic angle spinning (MAS) ^{13}C NMR spectroscopy and indirectly by analyzing the leaching water after polymerization via high performance liquid chromatography. The effect of MBA cross-linker on the mechanical strength, rheological behavior, and volume phase transition of P(NIPAAm-co-MBA) hydrogels was investigated.

2. Experimental

2.1. Materials

N-isopropylacrylamide (NIPAAm) (Acros Organics, Belgium, stabilized with 500 ppm p-methoxyphenol), *N*,*N*′-methylene-bis-acrylamide (MBA), ammoniumpersulfate (APS) and *N*,*N*,*N*′,*N*′-tetramethylethanediamine (TEMED) were supplied by Sigma-Aldrich, Germany and used as received. Chromatographic grade acetonitrile was obtained from Merck (Merck, Darmstadt, Germany). The high purity water was produced by Millipore system (Millipore, Billerica, USA).

2.2. Preparation of the gels

P(NIPAAm-co-MBA) hydrogels were prepared by redox free radical polymerization in water according to the method described by other authors [18, 19]. Briefly, to 5 ml aqueous solution of NIPAAm (1.0 M stock solution), the required quantity of MBA aqueous solution (0.1 M stock solution) was added resulting in an R value varying from 10 to 90 as indicated in Table 1. The quantity of APS and TEMED was 2 wt% respectively based on NIPAAm weight. The polymerization was performed in an ice-bath for 30 minutes, and left to stand for 72 hours at 25°C. After polymerization gels were washed in copious amount of deionized water at 25°C to remove the homopolymer and any unreacted components and all amount of the leaching water was collected. Gel purity was confirmed by testing the leaching water for residual monomers using UV-VIS spectroscopy (190–250 nm), and for PNIPAAm homopolymer by heating the leaching water to 50°C (above the phase transition temperature). No opacity of leaching water was experienced referring

Table 1. Feed and copolymer composition of P(NIPAAm-co-MBA) hydrogels determined by HPLC and by solid state ^{13}C CP MAS spectroscopy (R = mol NIPAAm/mol MBA)

Feed	R	10	30	50	70	90
	NIPAAm mole%	90.91	96.77	98.04	98.59	98.90
Copolymer by HPLC from leaching water	R	9.33	27.65	45.30	63.94	81.65
	NIPAAm mole%	90.32	96.51	97.84	98.46	98.79
Copolymer by HPLC from Soxhlet extract	R	9.81	29.77	49.51	70.43	86.72
	NIPAAm mole%	90.75	96.75	98.02	98.60	98.86
Copolymer by ^{13}C CP MAS NMR	R	9.65	22.15	42.48	49.51	83.03
	NIPAAm mole%	90.61	95.68	97.70	98.02	98.81

to the lack of PNIPAAm. Another series of the gels was purified after polymerization by Soxhlet extraction with water. The collected leaching water and the Soxhlet extracts were analyzed for NIPAAm and MBA content with high performance liquid chromatography (HPLC). This served as an indirect method for determining the real copolymer composition of the gels. The gels purified by leaching with water were dried at 50°C in vacuum until constant weight and directly tested for composition by ^{13}C solid state NMR spectroscopy.

2.3. Methods of characterization

2.3.1. High performance liquid chromatography

An integrated Hewlett Packard 1090 high performance liquid chromatograph (HPLC) was used with a UV detector (HP, Santa Alto, USA), at a detection wavelength of 220 nm. The column was BDS Hypersil C18 (100 × 4.6 mm, particle size 3 μm) purchased from Thermo Electron Corporation (Thermo Fisher Scientific Inc., Waltham, USA). The mobile phase used for chromatographic separation of NIPAAm and MBA was 5 v/v% of acetonitrile in high purity water. The collected leaching water was diluted with the mobile phase of the same volume. An isocratic elution technique was applied with a flow rate of 0.5 ml/min and an injected volume of 5 μl. Three parallel measurements were performed for each sample. A calibration graph was prepared using serial dilutions of 10, 30, 50, 70 and 100 μg/mL.

2.3.2. Solid state ^{13}C-NMR spectroscopy

The solid state magic angle spinning (MAS) ^{13}C spectra of the samples were recorded on a Varian NMR System (Varian Inc., Palo Alto, CA, U.S.A.) operating at ^{1}H frequency of 600 MHz with a Chemagnetics 3.2 mm narrow bore triple resonance T3 probe in double resonance mode. The ^{13}C spectra were measured with the cross polarization (CP) technique under the Hartmann-Hahn conditions [20] and a rotor spinning rate of 10 kHz. The proton π/2 pulse was 3 μs and ramped cross polarization was used. The contact time was 3 ms and SPINAL-64 proton decoupling with a power of 83 kHz was applied [21] during the acquisition. The dry network samples were manually grained and kept in a vacuum chamber at 50°C for one day before measurements. The presence of residual solvent was checked by one pulse proton spectra and all the samples were found to be free of remaining solvent molecules. The measuring temperature was 25°C and adamantane was used as the external chemical shift reference.

2.3.3. Dynamic rheometry

For rheological measurements an Anton Paar UDS 200 rheometer (Anton Paar GmbH, Graz, Austria) was used with a plate-plate arrangement. The distance of the plates was 0.5 mm. The dry gel samples were applied to the plate, deionised water was added, and equilibrium swelling was attained. Excess water was wiped with a tissue paper and after the sample thickness was adjusted, excess water was again added to the plate to avoid the loss of water from the sample during the measurements. Three parallel measurements were taken, on individual samples. For each of the samples, small deformation linearity was checked in the deformation range of 0.01–100 % strain amplitude at 10 Hz angular frequency at 25°C. Temperature sweeps were taken with the same arrangement between 25–60°C at 3°C·min^{-1} heating rate, 10 Hz angular frequency and 1% strain amplitude. Frequency sweeps were carried out at 25°C in the range of 0.1–600 Hz angular frequency and 1% strain amplitude. After the temperature sweeps a frequency sweep was taken at 60°C with the same arrangement.

2.3.4. Stress-strain measurements

Uniaxial compression modulus of the gels was measured by a single column mechanical tester using Instron 5543 equipment (Pulse Technology, Sonoma, CA, U.S.A.) with a load cell of 5 N. Cylindrical gels were prepared, and the measurements were performed after the gels achieved their swelling equilibrium in water at ambient temperature. The height and the diameter of the cylindrical test specimen were measured under water without load. Three samples of each kind of gels were measured. The elastic modulus, E, was determined from the slope of linear dependence described by Eqution (1) [22]:

$$\sigma = \frac{F}{A_0} = E(\lambda - \lambda^{-2}) \quad (1)$$

where σ is the applied stress, F is the value of measured force, A is the cross section of the undeformed swollen cylindrical gel, and λ is the relative deformation of the measured specimen.

3. Results and discussion

3.1. Copolymer composition

P(NIPAAm-co-MBA) copolymers with different monomer ratios (i.e. R varying from 90–10 corresponding to 90.9–98.9 mol% NIPAAm respectively) were synthesized by free radical polymerization in water solution with APS/TEMED as redox initiator system. In order to determine the yield of the polymerization reaction, the purified gels were weighed after drying. The yield was >95% in each case. All the gels appeared transparent and clear, except Gel R10, which was opaque. The copolymer composition of the gels was determined indirectly using HPLC analysis of the collected leaching water, as well as of the Soxhlet extracts, and directly by solid state NMR analysis of the dry gels.

3.1.1. Results of high-performance liquid chromatography

The retention times for MBA and NIPAAm were 5.54±0.01 and 9.02±0.01 minutes respectively for the applied chromatographic system. The other compounds used in the polymerization reaction (i.e. APS and TEMED) were not detected at the operating wavelength (220 nm). The detection limits for NIPAAm and MBA were calculated from the signal to noise ratio 3 to 1 and were found to be 160 and 332 ng/mL respectively. The selectivity of separation was proven by injection of blank solution and no signals were detected at the retention times of the solutes of interest.

NIPAAm monomer content (mol% and the corresponding 'R' values) in the feed and in the copolymer detected by HPLC analysis of the leaching water as well as of the Soxhlet extracts are given in Table 1. On heating the leaching water to 50°C, i.e. above the temperature of volume phase transition, no precipitation of the homopolymer PNIPAAm could be detected visually. For both series at high conversion the composition of the resulting copolymer is close to that of the monomer feed. This also means that the R values (the molar ratio of NIPAAm to MBA) in the feed closely approximates the composition of the formed polymer gels as found by HPLC analysis.

It should be noted that in the 2nd series of experiments Soxhlet extraction was used to purify the gels despite the temperature of purification being higher than the phase transition temperature. Gupta *et al*. [23] have also used Soxhlet extraction for removing ungrafted PNIPAAm homopolymer from grafted cellulose. It was expected that impurities become entrapped at higher cross-link ratio in the gel during Soxhlet purification, due to the high cross-link density, and collapsed structure of the gels during extraction. To test the presence of residual homopolymer trapped in the gels, gels were reversibly swelled (at room temperature) and shrunk in the leaching water following Soxhlet extraction. Surprisingly, neither homopolymer nor monomers could be detected by HPLC following the cooling-heating cycle. This perhaps could be attributed to the presence of some porosity in the network structure (even in the higher cross-link range, and with the temperature being above the LCST of PNIPAAm) which enabled the precipitated polymer to be released. However, due to the non-solubility of the homopolymer above the phase transition temperature, we do not recommend Soxhlet extraction for purification of PNIPAAm gels.

3.1.2. Results of NMR spectroscopy

Nuclear magnetic resonance spectroscopy is a unique and direct method to determine the composition of polymeric materials. From signal intensities of the different groups the composition can be determined with high accuracy. Unfortunately, for the P(NIPAAm-co-MBA) gels, the monomer and the cross-linker units display similar chemical structures. By analysis of the ^{1}H and ^{13}C solution state NMR spectra of the monomers, only the proton resonances of the CH_2 group of the MBA (4.6 ppm) was distinguishable from the signals of the main chain CH_2 groups. However, the proton spectra of the highly swollen polymer gels displayed broad lines and the resonances of the CH_2 group of MBA overlapped with that of the CH group of NIPAAm, and the former peak could not be deconvoluted. From the ^{13}C-NMR spectra the ratio of the carbonyl and methyl signal intensities enables the calculation of the composition. Due to inhomogeneities of the sample in the NMR tube, however, the ^{13}C signals were very broad (spectra not shown). To get a good carbon spectra in the liquid state several days are needed. By using the cross polarization technique in the solid state, the measuring time was dramatically shortened (3 h). The application of cross polarization technique combined with magic angle spinning of

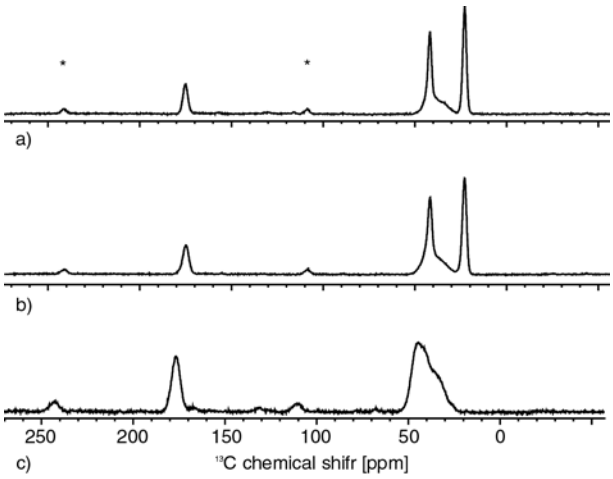

Figure 1. ^{13}C CP MAS spectra of (a) PNIPAAm, (b) P(NIPAAm-co-MBA) gel with 90.9 mole% NIPAAm (R = 10), and (c) poly(*N*,*N*′-methylene-bis-acrylamide) (PMBA). The asterisks denote the spinning sidebands of the carbonyl signal (ν_R = 10 kHz).

the rotors and proper decoupling method resulted in excellent carbon spectra with good resolution as shown in Figure 1.

The signal intensity in the cross polarization ^{13}C spectra depends on the cross polarization dynamics. The measuring parameters were chosen to get optimum signals for both the carbonyl and the methyl groups. At these polymeric networks the proton environment of the carbonyl groups is very similar. The measuring temperature was far below the glass transition temperature, so the mobility of the chains was very low and approximately the same in all investigated samples. With these approximations and using the ratio of the carbonyl and methyl signal intensities with cross polarization ^{13}C spectra, the composition of the P(NIPAAm-co-MBA) gels could be calculated with an accuracy of 2%.

Table 1 contains the copolymer composition determined by solid state magic angle spinning (MAS) ^{13}C-NMR. With respect to an accuracy of 2% of solid state ^{13}C CP MAS-spectroscopy, these results support the findings of HPLC analysis, namely that at high conversion the composition of the copolymer gels are close to the feed composition. The R values are very sensitive to the molar ratio of the co-monomers, therefore the deviations from the R values of the feed are higher than the those of the molar concentrations. For simplicity during further evaluations we will refer to the R values of the feed composition, such as R 10, 30, 50, 70 and 90.

In addition to determining the composition of the synthesized gels, the efficiency of the purification method could be verified by solid and liquid state NMR spectroscopy. On the proton spectra no signals belonging to solvent or other small molecules (such as MBA or TEMED) were detected. Additionally, in the ^{13}C chemical shift range of C–C double bonds (110–135 ppm) no signals were identified, indicating the absence of any residual monomer. It can be stated that the impurity content of the gels was less than 1–2% which is within the sensitivity range of the applied methods.

3.2. Dynamic rheometry

3.2.1. Strain-amplitude sweep of the gels of different cross-link density at constant frequency and temperature

The stability of the structure of viscoelastic materials is measured with increasing strain. This means the measurement at constant angular frequency (ω = 10 Hz) and temperature (25°C) with increasing controlled strain amplitude (γ). This measurement refers to the strength of the gels. Its aim is the determination of the threshold limit of linear viscoelasticity (LVE), in order to select the strain for further measurements. The change of storage (G') and loss modulus (G'') of the gels with strain-amplitude is given in Figures 2 and 3 respectively.

With the decrease of cross-linker (MBA) content (i.e. with increasing R) the storage modulus decreased. This is comprehensible, since the lower the concen-

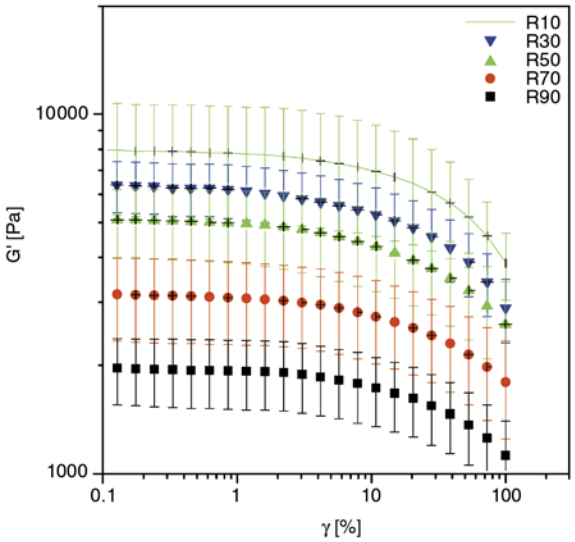

Figure 2. Change of storage modulus (G') with strain amplitude (γ) for P(NIPAAm-co-MBA) hydrogels with different cross-linker content (ω = 10 Hz, T = 25°C, n = 3)

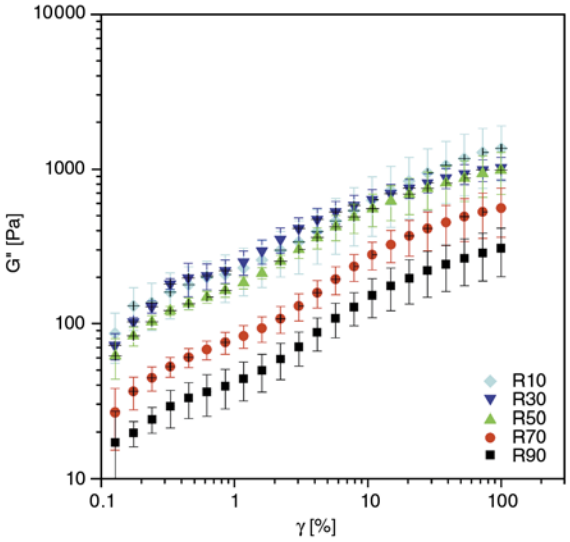

Figure 3. Change of loss modulus with strain amplitude for P(NIPAAm-co-MBA) hydrogels with different cross-linker content (ω = 10 Hz, T = 25°C, n = 3)

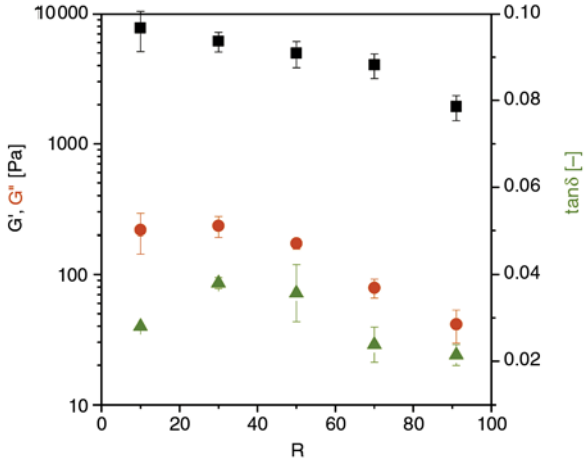

Figure 4. The change of storage modulus, loss modulus and damping factor with decreasing cross-linker content at γ = 1% strain amplitude (ω = 10 Hz, T = 25°C, n = 3)

tration of the network points, the easier the deformation of the gel. For gels R 10–50, however, the difference in storage modulus is significantly lower in the whole deformation range, than for the gels with lower cross-linker content (for gels R70 and 90). This may be attributed to the very loose network structure of these gels.

For all the gels the storage modulus remained constant with an increase in strain amplitude up until a threshold limit of the linear viscoelastic range, beyond which a sudden drop in storage modulus was observed for each gel (see Figure 2). As expected, the threshold limit of linear viscoelasticity (LVE) also decreases with decreasing cross-linker content (Table 2). For further measurements the strain amplitude γ = 1% was selected since all of the gels were still stable at this deformation.

In contrast to the change of storage modulus, the loss modulus continuously increases with increasing deformation. As for the storage modulus, the loss modulus was also dependent on the cross-link density, and in the whole range of deformation with decreasing cross-linker content (i.e. with increasing R) the loss modulus decreased. Hydrogels R10, R30 and R50 have practically identical loss modulus within the range of standard deviation, while hydrogels with less cross-linker content – R70 and R90 – have significantly lower loss modulus and their difference is also much higher. This fact also supports the assumption that the cross-link structure of gels R70 and R90 significantly differs from those with higher cross-linker content. Figure 4 shows the change of storage modulus, loss modulus and damping factor (tan δ = loss modulus/storage modulus) with varying cross-linker content selected at γ = 1% strain amplitude (ω =10 Hz at 25°C). With decreasing cross-linker content, i.e. with the increase of R, the moduli decrease. Above R70 the decrease in modulus is more pronounced. This is especially interesting, since in respect to the molar concentration gel R70 only slightly differs from R90 but the change is even more expressive than for gels with R10, 30 and 50 where there is much higher difference in the molar concentration of cross-linker. The loss factor (tan δ) decreases with decreasing cross-linker content, which may be attributed to the decreasing interaction between the polymer molecules. Gel R10 behaves anomalously, which may be caused by gel heterogeneity.

Table 2. Threshold limit of linear viscoelastic range of P(NIPAAm-co-MBA) hydrogels with different cross-linker content

Gel	Strain [%]	Storage modulus [Pa]	
		Average	St. dev.
R10	7.85	7143	2467
R30	5.73	5570	1022
R50	2.21	4863	1160
R70	1.89	3036	777
R90	1.61	1917	417

3.2.2. Temperature dependence of modulus with constant frequency and strain-amplitude

The change in storage modulus, loss modulus and in tan δ of all of the gels as a function of temperature is given in Figure 5. These measurements were carried out with controlled strain of 1%, and a frequency of 1 Hz.

As expected, below the temperature of volume phase transition the values of storage modulus are successively higher for the gels with higher cross-linker content. Up to the temperature of volume phase transition the storage modulus decreases with increasing temperature for all the gels. This may be understood by higher mobility and higher water uptake of the molecules with increasing temperature. The volume phase transition involves a dramatic increase in storage modulus for all of the gels (except R10) until equilibrium is reached. For gels R30–90 the volume phase transition involves a conformational change of the molecules from coil to globule, water is expelled and the more compact structure results in a dramatically higher storage modulus. The behaviour of Gel R10 is anomalous. This could be attributed to the higher MBA content in the R10 gel compared to the others. Due to the highest cross-linker concentration, the heat evolved during polymerization is higher, than for the gels with lower cross-linker content, resulting in local increase of the temperature above that of the phase transition leading to inhomogeneity. This is also supported by the opaque appearance of gel R10. Similarly to all the gels the volume phase transition of gel R10 starts at the same temperature (33°C), but it extends within a higher temperature range and the storage modulus does not increase after the phase transition. The reason for this may be the hindrance of conformation due to the high cross-link density. From the abrupt change of storage moduli the temperature of volume phase transition is in the range of 33–37°C, although this is not the most adequate parameter for its determination.

At the temperature of volume phase transition the loss moduli dramatically increase. Their onset temperature is almost identical for all the gels. With respect to the change of loss modulus with temperature Gel R10 also shows anomalous behaviour.

The most accurate method for determining the temperature of volume phase transition is monitoring the change of damping factor with temperature. Gels R70 and 90 are similar and have the lowest damping factor below and above phase transition. These are actually the best performing gels. The temperature of volume phase transition of the hydrogels determined from the change of rheological parameters with temperature is given in Table 3.

The cross-link density in the investigated range of MBA concentration (1.2–9.7 mol% in the copolymer) did not affect the temperature of volume phase

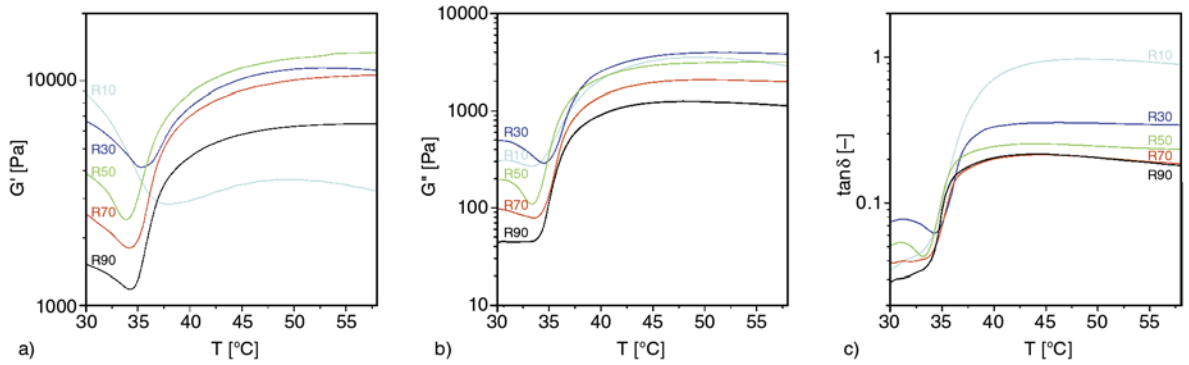

Figure 5. Change in storage modulus (a), loss modulus (b) and damping factor (tan δ) (c) with temperature for hydrogels with different cross-linker content (γ = 1%, ω = 1 Hz)

Table 3. Onset temperature of volume phase transition of P(NIPAAm-co-MBA) hydrogels with different cross-linker content from dynamic rheometry

Gel	From storage modulus		From loss modulus		From damping factor	
	Average	St. dev.	Average	St. dev.	Average	St. dev.
R10	33.1	0.7	32.3	0.1	32.5	0.5
R30	34.4	0.2	33.2	0.2	33.3	0.2
R50	33.2	0.3	33.0	0.2	33.0	0.1
R70	33.0	0.2	33.3	0.2	33.2	0.1
R90	33.8	0.5	33.3	0.6	33.0	0.1

transition, although 9.7 mol% MBA resulted in a broader temperature range of transition of Gel R10.

3.2.3. Frequency-sweep measurements at constant strain-amplitude below and above the temperature of volume phase transition

For presetting the strain with constant amplitude (γ = 1%), oscillatory measurements were carried out with increasing frequency (strain frequency sweep). These tests were conducted to verify the stability of the structures of viscoelastic materials below and above the phase transition temperature. The change of complex viscosity, storage modulus and loss modulus with angular frequency below and above the volume phase transition for the different hydrogels is represented in Figure 6.

The linear decrease of the complex viscosity with an increase in frequency is an indication of the cross-linked structure of the gels. The complex viscosity decreases with decreasing cross-linker content (with increasing R). Above the phase transition Gel R10 behaves anomalously just as in case of the temperature sweep. The reason may be heterogeneity and the differing gel structure due to the increased cross-link density. The mobility of the side chains of PNIPAAm is mostly hindered. Practically there is no change in the storage modulus with frequency below the phase transition, which refers to a stable, cross-linked structure. Above the phase transition the hydrophobic gels behave like polymers, meaning that the modulus slightly increases with increasing frequency for each gel, except for Gel R10, where a steep increase in storage modulus was observed. This may be due to a peculiar change in the structure of Gel R10 above phase transition temperature. Figure 7 represents the change of storage modulus, loss modulus and damping factor with cross-linker content from frequency sweep measurements at ω = 10 Hz at 25 and 60°C. Below the volume phase transition temperature the values of storage modulus are about two orders of magnitude higher than the values of the loss modulus, while above the phase transition temperature the difference between them is much lower. It follows that above the phase transition the loss modulus is impacted to a greater extent than the storage modulus. With decreasing cross-linker content both the storage and the loss modulus decrease.

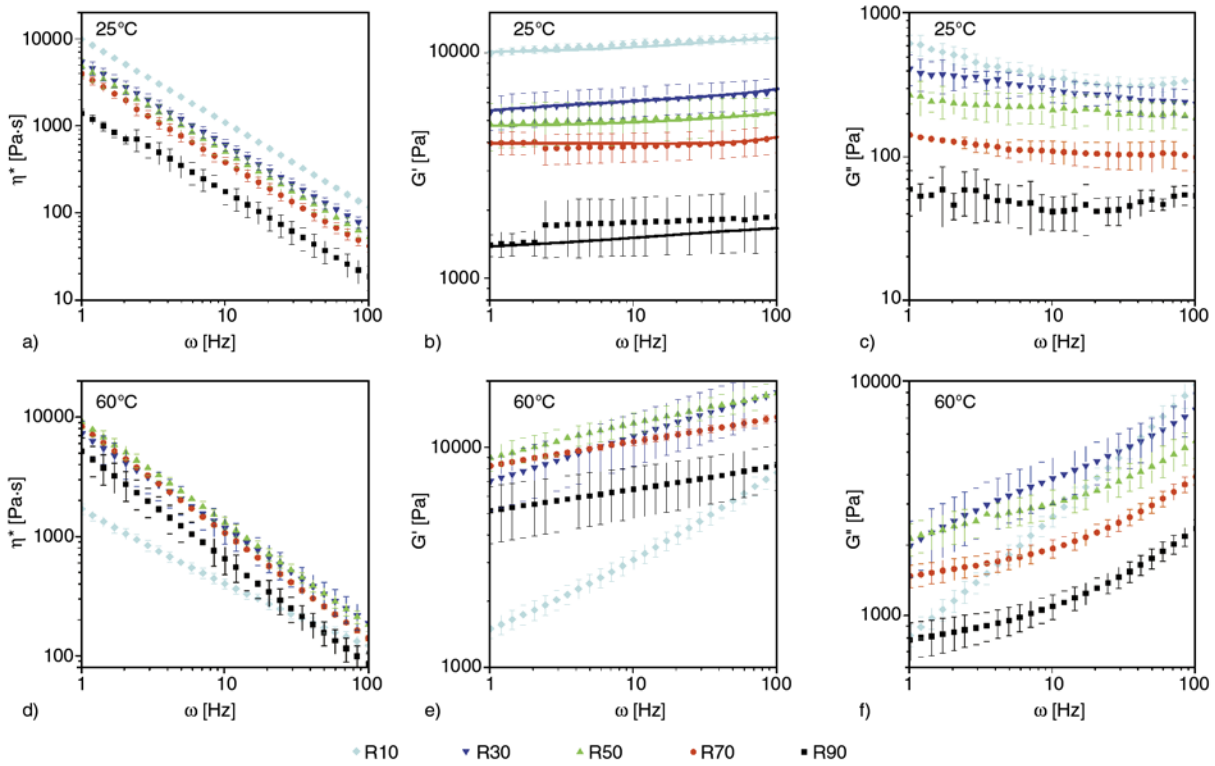

Figure 6. The change of complex viscosity(η^*) (a, d), storage modulus (G') (b, e) and loss modulus (G'') (c, f) at 25°C (a–c) and 60°C (d–f) for the gels with different cross-linker content (γ = 1%)

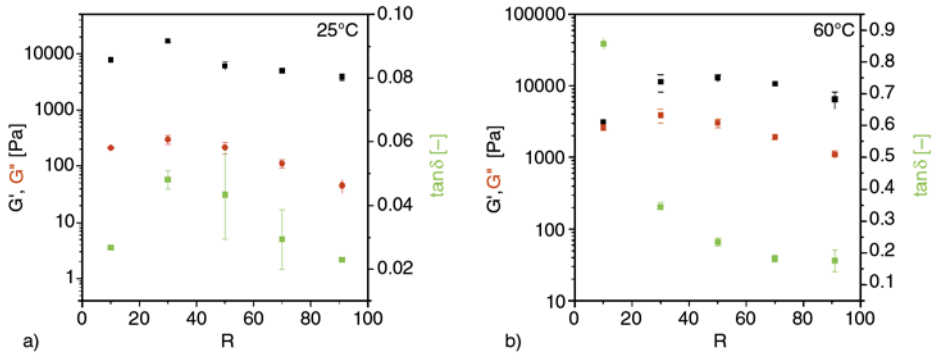

Figure 7. The change of storage modulus, loss modulus and damping factor (tan δ) with decreasing cross-linker content at 25 (a) and at 60°C (b) from frequency sweep measurements at 10 Hz angular frequency (γ = 1%)

3.3. Mechanical behaviour

Rheological characterization was completed with mechanical tests. Compressive elastic modulus of the gels was calculated and summarised in Table 4. Elastic modulus of the P(NIPAAm-co-MBA) hydrogels increased as the cross-linking density increased. Equilibrium swelling degree of hydrogels decreased as a function of cross-linking density. It presented a larger network density in the gels which caused an increased rigidity. Modulus of Gel R10 was anomalous, structure inhomogeneity appeared in a small modulus. In that case the modulus was not in correlation with the cross-linking density.

Table 4. Elastic modulus of P(NIPAAm-co-MBA) hydrogels with different cross-linker content

R	Elastic modulus [kPa]	
	Average	St. dev.
10	2.2	0.2
30	7.6	0.8
50	6.3	0.4
70	5.2	0.0
90	4.4	0.3

4. Conclusions

The composition of P(NIPAAm-co-MBA) copolymer hydrogels with varying cross-linker content in the range of 1.1–9.1 mol% MBA was determined. At high conversion (>95%) the composition of the copolymers was close to the feed composition as determined by HPLC analysis of the leaching water and Soxhlet extracts following polymerization. This was also confirmed by solid state ^{13}C CP MAS NMR spectroscopy of the formed gels. Due to the less accuracy of solid state NMR the R values calculated from the copolymer composition have higher deviations from those of the feed, since they are very sensitive to the molar concentration of the monomers.

At constant angular frequency with increasing controlled strain amplitude dynamic rheometry revealed that with the decrease of cross-linker (MBA) content (i.e. with increasing R) the storage modulus decreases. The threshold limit of linear viscoelasticity (LVE) also decreases with decreasing cross-linker content. The difference in both the storage and the loss moduli of hydrogels with the lowest cross-linker content (Gel R70 and R90) during strain amplitude sweep is much higher than those between the gels with higher cross-linker content. This significant difference may be attributed to the loose network structure of these gels (R70 and R90). By selecting the data from the strain amplitude sweep at γ = 1% and showing the change of storage modulus, loss modulus and damping factor with cross-linker content of the hydrogels, both storage and loss modulus decrease with decreasing cross-linker content. For hydrogels R90 and R70 the decrease in moduli is especially impressive. The damping factor (tan δ) decreases with decreasing cross-linker content, which may be attributed to the decreasing interaction between the polymer molecules.

The temperature dependence of the damping factor served the most accurate determination of the volume phase transition temperature of the hydrogels. The cross-link density in the investigated range of MBA concentration (1.2–9.7 mol% in the copolymer) did not affect the temperature of volume phase transition, although 9.7 mol% MBA resulted in a broader temperature range of transition of Gel R10 due to its anomalous behavior during the temperature sweep.

The frequency dependence of the complex viscosity, and storage modulus below and above the volume phase transition temperature support the stable

cross-linked structure of the hydrogels. Both complex viscosity, storage and loss modulus decrease with decreasing cross-linker content (increasing R). Gel R10 with the highest cross-linker content (9.7 mol% MBA in the copolymer) behaves anomalously due to heterogeneity and the hindered conformation of the side chains of PNIPAAm. Below the volume phase transition temperature the values of storage modulus are about two orders of magnitude higher than the values of the loss modulus, while above the phase transition temperature the difference between them is much lower. It may be concluded that above the phase transition temperature the loss modulus is impacted to a greater extent than the storage modulus.

Elastic modulus of the P(NIPAAm-co-MBA) hydrogels increased as the cross-link density increased. Modulus of Gel R10 was anomalously low due to structure inhomogeneity.

Acknowledgements

Authors thank the Hungarian Scientific Research Fund OTKA K75182, the Hungarian Science and Technology Foundation ZA-9/2006, the Hungarian project GVOP-3.2.1.-2004-04-0210/3.0, the National Science Foundation (South Africa), and the CSIR (South Africa), for financial support.

References

[1] Li P-F., Ju X-J., Chu L-Y., Xie R.: Thermo-responsive membranes with cross-linked poly(N-isopropyl-acrylamide) hydrogels inside porous substrates. Chemical Engineering and Technology, **29**, 1333–1339 (2006). DOI: 10.1002/ceat.200600174

[2] Fänger C., Wack H., Ulbricht M.: Macroporous poly (*N*-isopropylacrylamide) hydrogels with adjustable size 'cut-off' for the efficient and reversible immobilization of biomacromolecules. Macromolecular Bioscience, **6**, 393–402 (2006). DOI: 10.1002/mabi.200600027

[3] Lu Z-R., Kopečková P., Kopeček J.: Antigen responsive hydrogels based on polymerizable antibody fab' fragment. Macromolecular Bioscience, **3**, 296–300 (2003). DOI: 10.1002/mabi.200390039

[4] Zhang X. X., Li J., Gao J., Sun L., Chang W. B.: Determination of morphine by capillary electrophoresis immunoassay in thermally reversible hydrogel-modified buffer and laser-induced fluorescence detection. Journal of Chromatography A, **895**, 1–7 (2000).

[5] Zhang X-X., Li J., Gao J., Sun L., Chang W-B.: Determination of doping methyltestosterone by capillary electrophoresis immunological analysis with thermally reversible hydrogel and laser-induced fluorescence. Electrophoresis, **20**, 1998–2002 (1999). DOI: 10.1002/(SICI)1522-2683(19990701)20:10<1998::AID-ELPS1998>3.0.CO;2-C

[6] Haraguchi K., Takehisa T., Ebato M.: Control of cell cultivation and cell sheet detachment on the surface of polymer/clay nanocomposite hydrogels. Biomacromolecules, **7**, 3267–3275 (2006). DOI: 10.1021/bm060549b

[7] Cai W., Anderson E. C., Gupta R. B.: Separation of lignin from aqueous mixtures by ionic and nonionic temperature-sensitive hydrogels. Industrial and Engineering Chemistry Research, **40**, 2283–2288 (2001). DOI: 10.1021/ie0009435

[8] Kosik K., Wilk E., Geissler E., László K.: Distribution of phenols in thermoresponsive hydrogels. Macromolecules, **40**, 2141–2147 (2007). DOI: 10.1021/ma0624806

[9] László K., Kosik K., Rochas C., Geissler E.: Phase transition in poly(*N*-isopropylacrylamide) hydrogels induced by phenols. Macromolecules, **36**, 7771–7776 (2003). DOI: 10.1021/ma034531u

[10] Kosik K., Wilk E., Geissler E., László K.: Interaction of phenols with thermo-responsive hydrogels. Colloids and Surfaces A: Physicochemical and Engineering Aspects, **319**, 159–164 (2008). DOI: 10.1016/j.colsurfa.2007.07.022

[11] Hoare T. R., Kohane D. S.: Hydrogels in drug delivery: Progress and challenges. Polymer, **49**, 1993–2007 (2008). DOI: 10.1016/j.polymer.2008.01.027

[12] Chang D. P., Dolbow J. E., Zauscher S.: Switchable friction of stimulus-responsive hydrogels. Langmuir, **23**, 250–257 (2007). DOI: 10.1021/la0617006

[13] Yamashita K., Nishimura T., Ohashi K., Ohkouchi H., Nango M.: Two-step imprinting procedure of interpenetrating polymer network-type stimuli-responsive hydrogel-adsorbents. Polymer Journal, **35**, 545–550 (2003). DOI: 10.1295/polymj.35.545

[14] Sugiura S., Szilágyi A., Sumaru K., Hattori K., Takagi T., Filipcsei G., Zrínyi M., Kanamori T.: On-demand microfluidic control by micropatterned light irradiation of a photoresponsive hydrogel sheet. Lab on a Chip, **9**, 196–198 (2009). DOI: 10.1039/B810717C

[15] Petit L., Karakasyan C., Pantoustier N., Hourdet D.: Synthesis of graft polyacrylamide with responsive self-assembling properties in aqueous media. Polymer, **48**, 7098–7112 (2007). DOI: 10.1016/j.polymer.2007.09.040

[16] Senff H., Richtering W.: Influence of cross-link density on rheological properties of temperature-sensitive microgel suspensions. Colloid and Polymer Science, **278**, 830–840 (2000).
DOI: 10.1007/s003960000329

[17] Zeng F., Zheng X., Tong Z.: Network formation in poly(*N*-isopropyl acrylamide)/water solutions during phase separation. Polymer, **39**, 1249–1251 (1998).
DOI: 10.1016/S0032-3861(97)00471-0

[18] László K., Kosik K., Geissler E.: High-sensitivity isothermal and scanning microcalorimetry in PNIPA hydrogels around the volume phase transition. Macromolecules, **37**, 10067–10072 (2004).
DOI: 10.1021/ma048363x

[19] Zhang X., Zhuo R., Yang Y.: Using mixed solvent to synthesize temperature sensitive poly(N-isopropylacrylamide) gel with rapid dynamics properties. Biomaterials, **23**, 1313–1318 (2002).
DOI: 10.1016/S0142-9612(01)00249-6

[20] Hartmann S. R., Hahn E. L.: Nuclear double resonance in the rotating frame. Physical Review, **128**, 2042–2053 (1962).
DOI: 10.1103/PhysRev.128.2042

[21] Fung B. M., Khitrin A. K., Ermolaev K. J.: An improved broadband decoupling sequence for liquid crystals and solids. Journal of Magnetic Resonance, **142**, 97–101 (2000).
DOI: 10.1006/jmre.1999.1896

[22] Muniz E. C., Geuskens G.: Compressive elastic modulus of polyacrylamide hydrogels and semi-IPNs with poly(*N*-isopropylacrylamide). Macromolecules, **34**, 4480–4484 (2001).
DOI: 10.1021/ma001192l

[23] Gupta K. C., Khandekar K.: Temperature-responsive cellulose by ceric(IV) ion-initiated graft copolymerization of *N*-isopropylacrylamide. Biomacromolecules, **4**, 758–765 (2003).
DOI: 10.1021/bm020135s